Russian Journal of General Chemistry, Vol. 75, No. 5, 2005, pp. 700–707. Translated from Zhurnal Obshchei Khimii, Vol. 75, No. 5, 2005, pp. 742–750.

Molecular Structure and Conformational Preferences of Trimethyl Phosphorotrithioite, $P(SMe)_3$, Evaluated by Gas-Phase Electron Diffraction and Quantum Chemical Calculations

A. V. Belyakov*, A. N. Khramov*, P. E. Baskakova*, and V. A.Naumov**

** St. Petersburg State Technological Institute (Technical University), St. Petersburg, Russia*
*** Arbuzov Institute of Organic and Physical Chemistry, Kazan Research Center, Russian Academy of Sciences, Kazan, Tatarstan, Russia*

Received June 6, 2004

Abstract — Free $P(SMe)_3$ molecule was studied by gas electron diffraction (GED) and by B3PW91/6-311+G* (DFT) and MP2/6-31+G* calculations. Each conformer is characterized by three dihedral angles τ(CSP*lp*), where *lp* denotes the direction of the lone electron lone pair on the P atom. DFT calculations indicate that the most stable conformer is an *anti*,*gauche*+,*gauche*– (*ag*+*g*–) conformer of C_s symmetry; the next are the *ag*+*g*+ (ΔE = 2.5 kJ mol^{-1}), *g*+*g*+*g*+ (ΔE = 5.2 kJ mol^{-1}), and *aa*+*g*+ (ΔE = 12.5 kJ mol^{-1}) conformers. The MP2 calculations give the similar order, with the relative energies of 0.3, 4.3, and 10.6 kJ mol^{-1}, respectively. The experimental GED data agree well with the presence of only two conformers: χ(*ag*+*g*+) = 80(20)% and χ(*ag*+*g*–) = 20(10)%.

Thioesters of three-coordinate phosphorus acids strongly differ in the chemical behavior from their oxygen analogs [1, 2] whose structures and properties are studied quite comprehensively [3, 4]. However, the structures of thioesters, especially in the gas phase, are studied to a much lesser extent.

The goal of this study was to determine the molecular structure and conformational stability of gaseous $P(SMe)_3$ molecule by electron diffraction and quantum chemical calculations. For better understanding of the conformational preferences of the free molecule, we also included the calculation results for the F_2PSMe molecule.

The simplest molecules containing a single bond between P and S atoms, i.e., H_2PSH and F_2PSH, were studied by *ab initio* molecular orbital calculations in [5]. Each of them has stable conformations in which the S–H bond is located *syn*-periplanar and *anti*-periplanar relative to the lone electron pair of the P atom (P*lp*). It was found that the *syn* structure is preferred in the compound with equivalent substituents, whereas the *anti* form is preferred with different substituents. According to the IUPAC rules, the dihedral angle τ(HSP*lp*) describing the relative orientation of two terminal fragments of the molecules should be defined as 0° in *syn* and 180° in *anti* conformations [6].

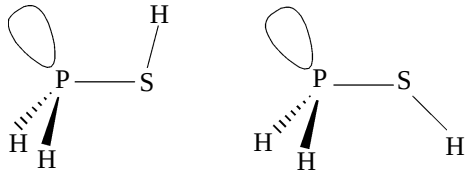

The related molecules with methyl groups, Me_2PSMe and F_2PSMe, were studied experimentally and theoretically in [5, 7–9]. As indicated above for the free molecules, the *syn* or approximately *syn* structure is preferred in the compound with equivalent substituents, whereas the *anti* form is preferred with different substituents. Unfortunately, Davis *et al*. [9] in an ED study of F_2PSMe failed to determine unambiguously the predominant conformation, probably due to existence of impurity in the sample.

The molecules of the series $MeSPX_2$ (X = Cl, Br) were studied by GED in [10, 11]. According to the experimental data, the *gauche* and *anti* forms equally well agree with the experiment. The results of our DFT calculations at the B3PW91/6-311+G* level indicate that, for the $MeSPCl_2$ molecule, the *anti* form is by 5.8 kJ mol^{-1} more stable than the *gauche* form.

The above example shows that, even in simple compounds with a single axis of internal rotation about the P–S bond, it is difficult to determine un-

1070-3632/05/7505-0700

ambiguously the conformation solely from the GED data, without using additional theoretical and experimental information.

The problem becomes much more complex in the case of molecules with two or three degrees of freedom of internal rotation. Very little is known about the conformational preferences of trimethyl phosphorotrithioite, $P(SMe)_3$. Taking into account that the electronegativity of the S atom is close to that of carbon, extrapolation based on the conformational properties of Me_2PSMe molecule suggests that the equilibrium conformation may be characterized by three methylthio groups in the *syn* or approximately *syn* orientation relative to the lone electron pair on the P atom. However, models with methylthio groups in other orientations should be considered also. Indeed, an early ED study of the $P(SMe)_3$ molecule showed that, in the gas phase, on the assumption of the local C_{3v} symmetry for the PS_3 groups, the compound exists as a mixture of three conformers with *gauche* and *anti* orientation of the methylthio groups relative to the lone electron pair on the P atom, with the *gauche-gauche-gauche* conformer of the C_3 symmetry prevailing [12]. To check and refine these conclusions, we decided to revise the previous ED data using additional data on the geometry and force fields of the molecules according to DFT and MP2 calculations. The preliminary results were published in [13].

Quantum-chemical calculations were carried out on the B3PW91/6-311+G* (DFT) and MP2/6-31+G* (MP2) levels of theory using the GAUSSIAN program system [14]. The structure optimization for the *anti* conformer of the F_2PSMe molecule was carried out assuming the C_s symmetry, and that of the *gauche* conformer, without imposing symmetry restrictions. The calculations of the molecular force fields confirmed that the optimal structures thus obtained correspond to the minima on the potential energy hypersurface. The structure optimization (DFT) for the $P(SMe)_3$ molecule without imposing symmetry restrictions revealed two nondegenerate minima; the structure optimization assuming C_s and C_3 symmetry followed by calculation of the force fields revealed two more minima. The MP2 geometry optimization followed by calculations of force constants for the C_s conformer, unlike the DFT method, revealed one imaginary frequency, which was preserved when using tighter convergence criteria, up to *Opt* = *VeryTight*. Nevertheless, the C_s conformer cannot be characterized as transition state, because it has one negative eigenvalue of the Hessian. Lowering the symmetry from C_s to C_1 and using the *Opt* = *VeryTight* convergence criterion resulted in the structure that was very close to that of the C_s symmetry with no imaginary frequencies but one very low frequency (17 cm^{-1}). Lowering of the symmetry may be due to numerical errors of the MP2 method.

The DFT theoretical molecular force fields were used to calculate the mean vibrational amplitudes (u) and vibrational correction terms $D = r_a - r_\alpha$ using a program from [15].

Gas electron diffraction. In our study we used the observed intensity curves recorded in [16]. The atomic scattering factors were taken from [17]. The experimental backgrounds were drawn as cubic spline functions to the difference between the experimental and theoretical molecular intensity curves using a program developed by A.V. Belyakov.

Least-squares structure refinements were carried out with a modified version (A.V.B.) of the program KCED25M [18, 19]. The weight matrices were diagonal; the long distance data were assigned unit weight, and the short distance data weight was 0.5. Estimated standard deviations calculated by the program were multiplied by a factor of three to include the added uncertainty due to data correlation and nonrefined vibrational amplitudes as well as an estimated scale uncertainty of 0.1%.

The three P–S, S–C, and C–H distances were refined as independent parameters; the differences between the chemically equivalent but symmetry-nonequivalent bond distances (e.g., P–S distances) in the same conformer or between chemically equivalent bond distances in different conformers were fixed at the values given by DFT calculation. Similarly, the mean SPS, PSC, and SCH bond angles were refined as independent parameters, while the differences between chemically similar but symmetry-nonequivalent angles were fixed at the calculated values. Three dihedral angles characterizing the rotation of the PSMe groups were refined as independent parameters for the predominant conformer *ag+g+*, while the dihedral angles in the other conformers were fixed at the values obtained from the DFT calculations. Methyl groups were assumed to be in staggered orientation. Finally, we refined the mole fractions of the ±*ag+g+* and *ag+g–* conformers, and the mole fraction of the ±*g+g+g+* conformer was calculated as the difference $\chi(\pm g+g+g+) = 1 - \chi(\pm ag+g+) - \chi(ag+g-)$; the mole fraction of the less stable ±*aa+g+* conformer was assumed to be equal to zero. In accordance with the experiment, to obtain the final geometry parameters, the mole fraction $\chi(\pm g+g+g+)$ was fixed at zero. The mean amplitudes for the P–S, S–C, and C–H bonds and the amplitudes for nonbonded distances were refined in groups with constant fixed differences. The total number of simultaneously refined

Table 1. Structural parameters of the F_2PSMe molecule, determined at the B3PW91/6-311+G* (DFT) and MP2/6-31+G*[a] levels of theory

Parameter	DFT		MP2	
	anti	*gauche*	*anti*	*gauche*
Bond distance				
P–F	1.626	1.623/1.616[b]	1.635	1.631/1.625[b]
P–S	2.105	2.115	2.083	2.093
S–C	1.828	1.829	1.824	1.826
Bond angle				
SPF	100.9	102.6/96.9[c]	100.6	102.7/97.0[c]
FPF	94.8	96.2	94.8	96.1
PSC	102.6	97.0	101.8	97.0
Dihedral angle				
CSP*lp*	180	–33.8	180	–31.8
CSPF	±48.6	99.7/–162.3[d]	±48.5	101.8/–160.3[d]
Relative energy ΔE	0	6.1	0	10.5

[a] The bond distances are in Å; angles, in degrees; relative energies ΔE, in kJ mol^{-1}. [b] P–F^1/P–F^2; for the numbering of F atoms in the *gauche* conformer, see Fig. 1. [c] SPF^1/SPF^2. [d] τ(CSPF1)/τ(CSPF^2).

independent parameters was 14, including two scale factors.

When refining structural parameters (bond lengths *r*, mean amplitudes of vibrations of atom pairs *u*, etc), the minimized functional has the form:

$$Q = \sum_s w_s \Delta_s^2 = \Sigma w_s [sM^{obs}(s) - ksM^{cal}(s)]^2, \quad (1)$$

where w_s is a weight function; $s = (4\pi/\lambda)\sin(\theta/2)$, parameter of scattering angle θ; λ, wavelength of electron beam; $sM(s)$, molecular intensity curve; and *k*, scale factor. As a criterion of minimum of the functional serves the *R*-factor:

$$R = (Q/\sum_s w_s [sM^{obs}(s)]^2)^{1/2}. \quad (2)$$

Conformational preferences and anomeric effects in F_2PSMe molecule. The DFT and MP2 calculations of a simpler F_2PSMe molecule were carried out for better understanding of the structure and conformational preferences in the A_2PSMe fragment, where A is an electronegative element with stronger anomeric effects than in the $P(SMe)_3$ molecule.

The structure optimization for F_2PSMe revealed two distinct conformers, the most stable of them being *anti* conformer of the C_s symmetry, shown in Figs. 1a and 1b. The calculations revealed also two degenerate minima corresponding to two enantiomeric *gauche* conformers of C_1 symmetry at the higher energy (Figs. 1c, 1d). The structural parameters corresponding to the refined models are given in Table 1.

We have previously suggested that the equilibrium conformers of aminophosphanes, A_2PNMe_2, are stabilized by anomeric effects, i.e., through delocalization of the lone electron lone pair of N to antibonding P–A orbitals [20, 21]. Therefore, we decided to analyze such effects in the F_2PSMe molecule by natural bond orbital (NBO) analysis [22] (Fig. 1, Table 2). Such analysis of the wavefunction of the *anti* conformer indicates that anomeric delocalization of the lone electron pair of the P atom to the antibonding σ^*(S–C) orbital (Fig. 1a) stabilizes this conformer by approximately 4.7 kJ mol^{-1}. The delocalization energy is expected to reach a maximum at the dihedral angle τ(*lp*PSC) = 180° and to be at minimum when this angle is about 90°; in the *gauche* conformer, where τ(*lp*PSC) = –34°, it already decreases almost to zero.

The relative orientation of the PF_2 and SMe fragments in the *gauche* conformer is such that the direction of the πlp of the S atom is nearly coplanar with the P–F^1 bond and nearly perpendicular to the P–F^2 bond (Fig. 1d). As a consequence, the $\pi lpS \rightarrow \sigma^*[PF^1]$ stabilization energy is about 43.0 kJ mol^{-1}, while the $\pi lpS \rightarrow \sigma^*[PF^2]$ energy is only 6.7 kJ mol^{-1}. The former interaction causes the strongest anomeric stabilization of this conformer. It should be noted that the structural consequences of the anomeric effect are similar to those of conjugation of multiple bonds separated by a single bond. Indeed, the P–F^1 bond in the *gauche* conformer, according to the calculations, is approximately 0.6–0.7 pm longer than the P–F^2 bond, and the SPF^1 angle is approximatley 6° larger than the SPF^2 angle. In the *anti* conformer, πlp of the S atom interacts equally with both σ^*(P–F) orbitals (Fig. 1b); this delocalization stabilizes the *anti* conformer by 55 kJ mol^{-1}. Like the anomeric delocalization of the *lp* of P, the delocalisation of πlpS stabilizes the *anti* conformer relative to the *gauche* conformer. The σlp of the S atom is more tightly bound than the πlp, and the anomeric delocalization energies are much lower (Table 2). The anomeric delocalization of three lone pairs *lp*P, σlpS, and πlpS along the P–S bond stabilizes in total the *anti* conformer by 60 and the *gauche* conformer by 55 kJ mol^{-1}. The difference between these stabilization energies of 5 kJ mol^{-1} is close to the difference in the electronic energies between the *anti* and *gauche* conformers, ΔE =

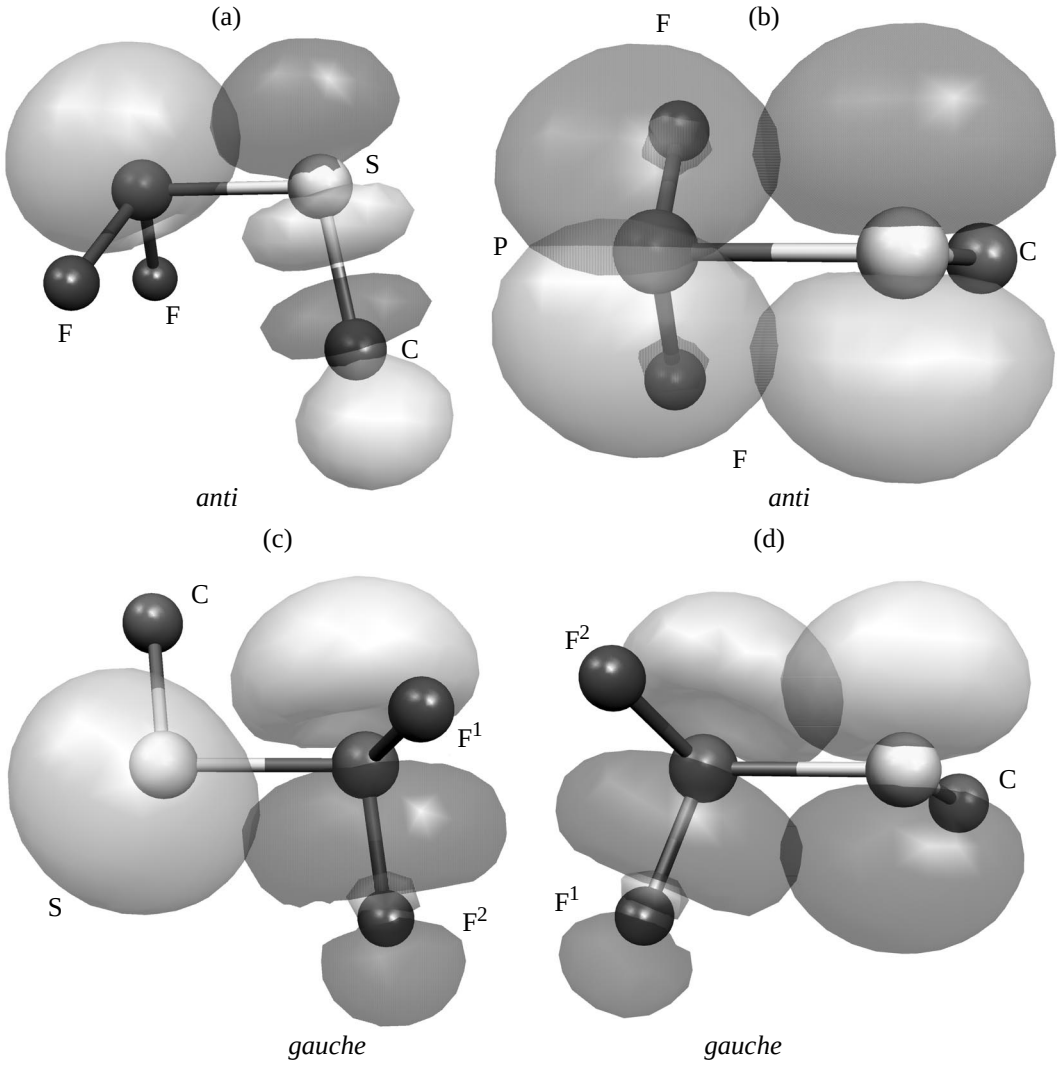

Fig. 1. Anomeric effects in the *anti* and *gauche* conformers of the F_2PSMe molecule. The symmetry of the *anti* conformer is C_s. (a) Delocalization of the P*lp* to the C–S antibonding orbital; (b) delocalization of the πlp of S to the two PF_2 antibonding orbitals (the less stable *gauche* conformer has the C_1 symmetry); (c) Delocalization of the σlp of S to the PF^2 antibonding orbital; (d) delocalization of the πlp of S to the PF^1 antibonding orbital.

6 kJ mol^{-1}. Delocalization of each of the three lone pairs is expected to strengthen and thus shorten the P–S bond, and we note that the P–S bond distance calculated for the *anti* conformer is indeed approximately 1 pm shorter than in the *gauche* conformer. The similar results were obtained in the NBO analysis of the F_2POMe molecule [23]. The results of NBO analysis are thus fully consistent with the assumption that both the conformational stabilities and bond distances and bond angles in the two conformers are determined by anomeric effects.

Molecular structure and conformational preferences of the $P(SMe)_3$ molecule, according to quantum chemical calculations and gas electron diffraction. DFT calculations at the B3PW91/6-311+G* level and MP2/6-31+G* calculations revealed four nondegenerate minima on the potential energy surface, corresponding to four different molecular conformations shown in Fig. 2. A ball-and-stick model with atoms numbering of the *ag+g+* conformer of the C_1 symmetry that gives the best fit to the experimental data is shown in Fig. 3. The relative electronic energies at 0 K and the relative standard enthalpies and Gibbs free energies at 298 K are listed in Table 3 together with bond distances, bond angles, and dihedral angles.

Table 2. Anomeric effects in the *anti* and *gauche* conformers of the F_2PSMe molecule and in each $(S_2)PSMe$ fragment of the *ag*+*g*+ conformer of the $P(SMe)_3$ molecule[a]

Conformer or fragment	F_2PSMe						
	τ(*lp*PSC)	Δε[*lp*P → σ*(S–C)]	τ(σ*lp*SPF)	Δε[σ*lp*S → σ*(PF$_2$)]	τ(π/*p*SPF)	Δε[π/*p*P → σ*(PF$_2$)]	ΣΔε
anti	180	4.7	±131	0.0	±41	27.5 + 27.5 = 55	59.7
gauche	–34	0.0	–80/18	0.0 + 5.4 = 5.4	10/–72[b]	43 + 6.7 = 49.7	55.1
	$(MeS)_2PSMe$						
	τ(*lp*PSC)	Δε[*lp*P → σ*(S–Cl)	τ(σ*lp*SPS')	Δε[σ*lp*S → σ*(PS')]	τ(π/*p*SPS')	Δε[π/*p*P → σ*(PS')]	ΣΔε
$(S'_2)PSC^1$	179	7.5	131/–126	3.3 + 0.0 = 3.3	41/–36	23.8 + 22.2 = 46.0	56.8
$(S'_2)PSC^2$	42	0.0	91/–14	0.0 + 0.0 = 0.0	2/76	37.2 + 0.0 = 37.2	37.2
$(S'_2)PSC^3$	42	0.0	–12/96	0.0 + 0.0 = 0.0	78/6	0.0 + 31.4 = 31.4	31.4

[a] The dihedral angles τ [in degrees] and *lp* → σ* delocalization energies (Δε) [in kJ mol^{-1}] were obtained by NBO analysis [22].
[b] P–F^1/P–F^2; for numbering of F atoms in the *gauche* conformer, see Fig. 1.

We shall characterize each conformer through the dihedral angles τ(CSP*lp*), where *lp* is the direction of the lone electron pair of the phosphorous atom; this lone pair is assumed to coincide in the direction with a normal to the plane passing through the three points located at unit distances along bonds around the P atom.

We found that, as in the case of the $ClP(SMe)_2$ molecule [24], the relative energies of the *ag*+*g*– conformer of C_s symmetry depend on the level of theory (Table 3). As follows from the results of MP2/6-31+G* calculations, the *ag*+*g*– conformer of the C_s symmetry is by only 0.6 kJ mol^{-1} more stable than the *ag*+*g*+ conformer of the C_1 symmetry (Table 3). In this case, to obtain more accurate result, it is necessary to use as high level of theory as possible. The *ag*+*g*– conformer has very low frequency of the

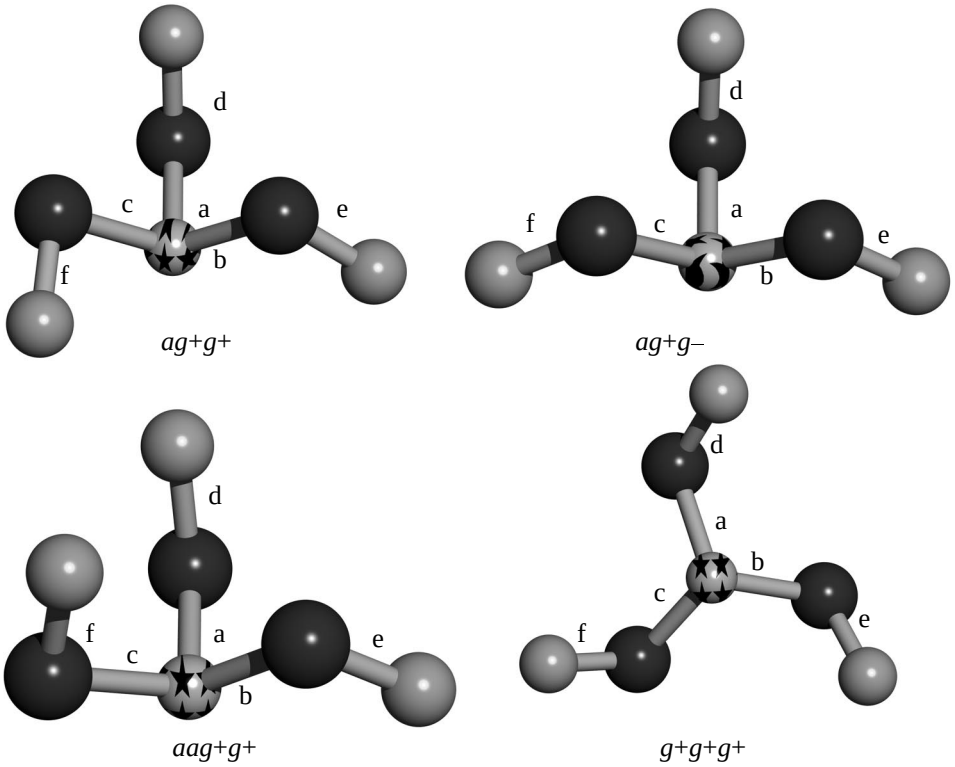

Fig. 2. Molecular conformations of the $P(SMe)_3$ molecule, as predicted by quantum chemical calculations, with designation of bonds.

Table 3. Experimental and calculated data for the $P(SMe)_3$ molecule[a]

Parameter	DFT/MP2				GED[b]	
	ag+*g*– (C_s)	*ag*+*g*+ (C_1)	*g*+*g*+*g*+ (C_3)	*aa*+*g*+ (C_1)	*ag*+*g*+ (C_1)	*ag*+*g*– (C_s)
ΔE	0/0	2.5/0.6	5.2/4.3	12.5/10.6	χ(*ag*+*g*–)	0.2(1)
ΔH^0_{298}	0/0	2.6/0.7	5.2/4.4	12.7/10.8	$\chi(\pm ag+g+)$[c]	0.8(2)
ΔG^0_{298}	0/0	3.6/3.1	6.8/7.5	14.9/14.8	$\chi(\pm g+g+g+)$[c,d]	0
χ	0.77/0.75	0.18/0.21[c]	0.05/0.04[c]	0.0/0.0[c]	$\chi(\pm aa+g+)$[c]	[0]
Bond length	r_e	r_e	r_e	r_e	r_a	r_a
P–S[1] [a][e]	2.146	2.129/2.107	2.143	2.139	2.106(32)	2.123(32)
P–S[2] [b]	2.145	2.154/2.130	2.143	2.147	2.130(32)	2.121(32)
P–S[3] [c]	2.145	2.143/2.122	2.143	2.134	2.120(32)	2.121(32)
S–C[1] [d]	1.821	1.823/1.820	1.824	1.821	1.831(70)	1.828(70)
S–C[2] [e]	1.823	1.824/1.820	1.824	1.823	1.832(70)	1.831(70)
S–C[3] [f]	1.823	1.823/1.819	1.824	1.826	1.831(70)	1.831(70)
C–H [f]	1.091	1.091/1.092	1.091	1.091	1.198(12)	1.198(12)
Bond angle	$\angle_e$	$\angle_e$	$\angle_e$	$\angle_e$	$\angle_a$	$\angle_a$
PSC[1] [ad]	105.2	105.7/105.0	98.4	107.7	104.4(27)	103.9(27)
PSC[2] [be]	97.4	98.2/97.4	98.4	97.5	96.9(27)	96.1(27)
PSC[3] [cf]	97.4	98.2/97.6	98.4	108.8	96.9(27)	96.1(27)
S^1PS^2 [ab]	106.0	106.2/106.3	100.3	105.8	105.6(8)	105.4(8)
S^1PS^3 [ac]	106.0	101.3/101.3	100.3	109.5	100.7(8)	105.4(8)
S^2PS^3 [bc]	94.7	98.9/99.5	100.3	100.3	95.5(12)	91.4(12)
SCH(*anti*)[f]	107	106/107	106	107	109	109
SCH(*gauche*)[f]	111	111/111	111	111	113	113
Dihedral angle	τ_e	τ_e	τ_e	τ_e	τ_a	τ_a
τ_a = C^1SPlp [da*lp*]	180.0	180.0/178.3	36.9	180.0	180.0(110)	180.0
τ_b = C^2SPlp [eb*lp*]	48.4	42.0/41.4	36.9	44.5	57.7(110)	64.2[d]
τ_c = C^3SPlp [fc*lp*]	–48.4	40.6/44.3	36.9	154.8	71.4(110)	–64.2
C^1SPS^2 [dab]	–49.9	–49.3/–50.8	–91.8	–51.4	–47.2(8)	–47.9(8)
C^1SPS^3 [dac]	49.9	53.7/52.7	165.6	55.8	51.6(8)	47.9(8)
C^2SPS^1 [eba]	–81.7	–88.0/–88.9	165.6	–80.4	–75.1(170)	–67.9(170)
C^2SPS^3 [ebc]	170.2	166.4/166.3	–91.8	165.5	–177.8(170)	–174.3
C^3SPS^1 [fca]	81.7	167.6/170.0	–91.8	–80.8	–160.1(102)	67.9
C^3SPS^2 [fcb]	–170.2	–83.8/–81.2	165.6	30.1	–53.1(170)	174.3

[a] First four columns: nondegenerate minima on the potential energy surface of the $P(SMe)_3$ molecule obtained by DFT calculations at the B3PW91/6-311+G* level (numerator) and by MP2/6-31+G* calculations (denominator). Relative electronic energies at 0 K (ΔE, kJ mol^{-1}), relative standard enthalpies (ΔH^0_{298}, kJ mol^{-1}), relative standard free energies (ΔG^0_{298}, kJ mol^{-1}) and mole fractions (χ) in the gas phase at 298 K; bond lengths in Å, bond angles and dihedral angles in degrees. Last two columns: mole fractions of the conformers; bond lengths, bond angles, and dihedral angles of the *ag*+*g*+ and *ag*+*g*– conformers obtained by least-squares refinement to the gas electron diffraction data. The electronic energy of the *ag*+*g*– conformer is –1655.5835/–1653.0083 au (1 au = 627.5 kcal mol^{-1}. [b] *R*-factor, 5.8%, was calculated by Eq. (2). [c] Racemic mixture. [d] Fixed in accordance with the experiment. [e] See Figs. 2 and 3. [f] Mean value.

torsional vibrations of the *gauche* fragments around the P–S bonds. This results in a large entropy contribution to the Gibbs free energy and in increased calculated mole fraction of this conformer. In so doing, it should be remembered that, for large-amplitude motions, the approximation of small harmonic vibrations may lead to significant errors. For the *ag*+*g*– model of the C_s symmetry, the MP2/6-31+G* calculations revealed one imaginary frequency, preserved at the *VeryTight* convergence criterion. The Hessian matrix had one negative eigenvalue. This indicates that the precise value of the energy minimum is, nevertheless, not reached yet. Lowering of the symmetry to C_1 with the *VeryTight* convergence criterion results in the absence of imaginary frequencies, but one normal frequency was very low, about 17 cm^{-1},

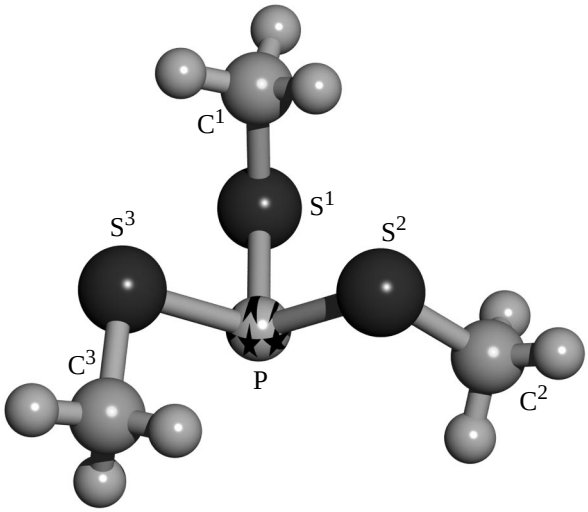

Fig. 3. A ball-and-stick model of the *ag*+*g*+ conformer of the $P(SMe)_3$ molecule, with atom numbering.

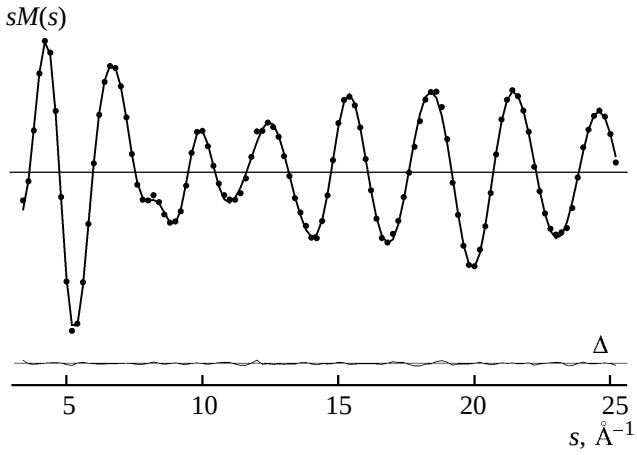

Fig. 4. Experimental (dots) and calculated (solid line) molecular intensity curves of the $P(SMe)_3$ molecule. Below is the difference curve (Δ).

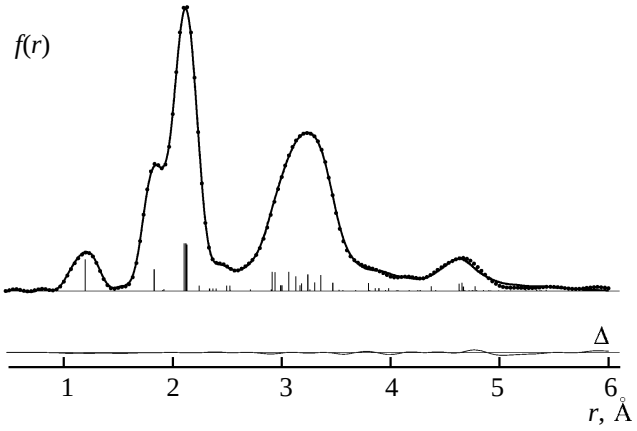

Fig. 5. Experimental (dots) and calculated (solid line) radial distribution curve of the $P(SMe)_3$ molecule. Below is the difference curve.

and the final optimized geometry parameters were very close to those of C_s symmetry model. Obviously, in this case the deviations of the *ag*+*g*– model from the C_s symmetry are due to the numerical errors of the MP2/6-31+G* method (Δ).

The *ag*+*g*+ conformer, which has C_1 symmetry, is optically active, and the enantiomer with dihedral angles of opposite sign would be equally stable. Optical enantiomers are indiscernible by gas electron diffraction. In what follows, we shall denote the racemic mixture of *ag*+*g*+ and *ag*–*g*– as ±*ag*+*g*+. The *ag*+*g*– conformer of the C_s symmetry is optically inactive. Note that the two *gauche* SMe groups are oriented oppositely to each other. The third (*aa*+*g*+) and fourth (*g*+*g*+*g*+) conformers are optically active; we shall denote their racemic mixtures as ±*aa*+*g*+ and ±*g*+*g*+*g*+.

Least-squares structure refinements were based on the assumption that χ(±*aa*+*g*+) = 0, because, according to the calculations, their mole fractions are negligible. Experimental data proved considerable prevalence of the *ag*+*g*+ conformer of the C_1 symmetry and presence of a small amount of the *ag*+*g*– conformer of the C_s symmetry, but the presence or absence of the *g*+*g*+*g*+ conformer of the C_3 symmetry could not be determined reliably (Table 3). The molecular intensity and radial distribution curves for the best set of geometric parameters from Table 3 are shown in Figs. 4 and 5.

The results of the NBO analysis of the anomeric effects in the *ag*+*g*+ conformer of the C_1 symmetry are given in Table 2. It is seen that the energy of anomeric stabilization due to donation of the P*lp* to the S–C antibonding orbital of the *anti*-methylthio group of the $P(SMe)_3$ molecule is even larger than that computed for the *anti* conformer of the F_2PSMe molecule, while the *lp*P → σ*(S–C) stabilization energies computed for the *gauche*-methylthio groups, as in the *gauche* conformer of the F_2PSMe molecule, are zero. As expected, the PSC bond angle of the *anti* group is approximately 8° larger than that computed for the *gauche* conformer.

The energies of anomeric stabilization in the $P(SMe)_3$ molecule due to the donation of the σ or π lone electron pairs of the S atoms to the antibonding orbitals of the opposite P–S' bonds are similar to those calculated for the corresponding conformer of the F_2PSMe molecule, except that in the $P(SMe)_3$ molecule the σ*lp*S → σ*(P–S') anomeric effect stabilizes the *anti* PSMe group, whereas the corresponding effect in the F_2PSMe molecule stabilizes the *gauche* conformer. Moreover, the strongest anomeric effects are associated with the π*lp*S → σ*(P–S') delocaliza-

tions. It should be noted that the anomeric delocalization of three lone pairs along the $P–S^1$ bond of the *anti* fragment of the $P(SMe)_3$ molecule stabilizes the *ag+g+* conformer by approximately 57 kJ mol^{-1}, whereas the stabilizations along the $P–S^2$ and $P–S^3$ bonds of the *gauche* fragments are approximately 20–25 kJ mol^{-1} smaller. As in the F_2PSMe molecule, we find that the stronger total anomeric delocalization is associated with the shorter bond. It would be logical from the viewpoint of anomeric effects that the second PSMe fragment be located in the *anti* position also. However, in this case, obviously, the steric repulsions between them will increase the energy. Indeed, although NBO analysis indicates that the anomeric stabilization of the *aa+g+* conformer is greater than that of the *ag+g+* conformer, the former is by approximately 10 kJ mol^{-1} less stable than the latter.

The calculated P–S bond lengths and PSC bond angles in the other conformers of the $P(SMe)_3$ molecule are equally consistent with the results obtained by NBO analysis of the anomeric effects. Thus, even though bond distances and bond angles in four conformers of the $P(SMe)_3$ molecule are consistent with the anomeric effects indicated by NBO analysis, their relative energies are determined not by anomeric effects alone but by a superposition of anomeric and steric interactions.

REFERENCES

1. Divinskii, A.F., Kabachnik, M.I., and Sidorenko, V.V., *Dokl. Akad. Nauk SSSR,* 1948, vol. 60, no. 6, p. 999.
2. Ofitserov, E.N., Sinyashin, O.G., Ivasyuk, N.V., Batyeva, E.S., and Pudovik, A.N., *Zh. Obshch. Khim.*, 1980, vol. 50, no. 6, p. 1217.
3. Vilkov, L.V. and Sadova, N.I., *Nitrogen and Phosphorous Compounds*, Hargittai, I. and Hargittai, M., Eds., New York: VCH, 1988, part B, p. 35.
4. Naumov, V.A. and Vilkov, L.V., *Molekulyarnye struktury fosfororganicheskikh soedinenii* (Molecular Structures of Organophosphorus Compounds), Moscow: Nauka, 1986.
5. Korn, M., Oberhammer, H., and Minkwitz, R., *J. Mol. Struct.*, 1993, vol. 300, no. 1/3, p. 61.
6. *Pure Appl. Chem.*, 1976, vol. 45, p. 11.
7. Durig, J.R., Barron, D.A., Sullivan, J.F., Anderson, D.G., Cradock, S., and Rankin, D.W.H., *J. Mol. Struct.*, 1992, vol. 268, no. 1/3, p. 143.
8. Durig, J.R. and Xiao, J., *J. Mol. Struct.*, 2000, vol. 526, no. 1/3, p. 373.
9. Davis, M.J., Rankin, D.W.H., and Cradock, S., *J. Mol. Struct.*, 1990, vol. 238, no. 1/3, p. 273.
10. Naumov, V.A., Kataeva, O.V., and Sinyashin, O.G., *Zh. Strukt. Khim.*, 1984, vol. 25, no. 3, p. 79.
11. Kataeva, O.V., *Cand. Sci. (Chem.) Dissertation*, Kazan, 1984.
12. Kataeva, O.N. and Naumov, V.A., *Zh. Strukt. Khim.*, 1987, vol. 28, no. 5, p. 153.
13. Belyakov, A.V., Khramov, A.N., and Naumov, V.A., Abstracts of Papers, *Twentieth Austin Symp. on Gas Phase Molecular Structure*, Austin, 2004, p. 92.
14. Frisch, M.J., Trucks, G.W., Schlegel, H.B., Scuseria, G.E., Robb, M.A., Cheeseman, J.R., Zakrzewski, V.G., Montgomery, J.A., Stratmann, R.E., Jr., Burant, J.C., Dapprich, S., Millam, J.M., Daniels, A.D., Kudin, K.N., Strain, M.C., Farkas, O., Tomasi, J., Barone, V., Cossi, M., Cammi, R., Mennucci, B., Pomelli, C., Adamo, C., Cliford, S., Ochterski, J., Petersson, G.A., Ayala, P.Y., Cui, Q., Morokuma, K., Malick, D.K., Rabuck, A.D., Raghavachari, K., Foresman, J.B., Cioslowski, J., Ortiz, J.V., Baboul, A.G., Stefanov, B.B., Liu, G., Liashenko, A., Piskorz, P., Komaromi, I., Gomperts, R., Martin, R.L., Fox, D.J., Keith, T., Al-Laham, M.A., Peng, C.Y., Nanayakkara, A., Gonzalez, C., Challacombe, M., Gill, P.M.W., Johnson, B., Chen, W., Wong, M.W., Andres, J.L., Gonzalez, C., Head-Gordon, M., Replogle, E.S., and Pople, J.A., *GAUSSIAN-98*, Rev. A.7, Pittsburgh: Gaussian, 1998.
15. Sipachev, V.A., *Advances in Molecular Structure Research*, Hargittai, I. and Hargittai, M., Eds., Greenwich: JAI, 1999, vol. 5, p. 323.
16. Tuzova, L.L., Naumov, V.A., Galliakberov, R.M., Ofitserov, E.N., and Pudovik, A.N., *Dokl. Akad. Nauk SSSR*, 1981, vol. 256, no. 4, p. 891.
17. Ross, A.W., Fink, M., and Hilderbrandt, R.L., *International Tables for Crystallography*, Dordrecht: Kluwer Academic, 1992, vol. C, p. 245.
18. Gundersen, G., Seip, H.M., and Strand, T.G., *The Norwegian Electron Diffraction Group. Annual Report*, Oslo: Univ. of Oslo, 1981, p. 8.
19. Gundersen, G., Samdal, S., and Seip, H.M., *Least Squares Structural Refinement Program Based on Gas Electron-Diffraction Data*, Oslo: Univ. of Oslo, 1980–1981, parts I–III.
20. Belyakov, A.V., Haaland, A., Shorokhov, D.J., Sokolov, V.I., and Swang, O., *J. Mol. Struct.*, 1998, vol. 445, no. 1/3, p. 303.
21. Baskakova, P.E., Belyakov, A.V., Colacot, T., Krannich, L.K., Haaland, A., Volden, H.V., and Swang, O., *J. Mol. Struct.*, 1998, vol. 445, no. 1/3, p. 311.
22. Weinhold, F. and Landis, C.R., *Chem. Ed.: Res. Pract. Eur.*, 2001, vol. 2, p. 91.
23. Belyakov, A.V., Dalhus, B., Haaland, A., Shorokhov, D.J., and Volden, H.V., *J. Chem. Soc., Dalton Trans.*, 2002, no. 3, p. 3756.